

# DESIGN AND IMPLEMENTATION OF A MPPT USING FUZZY LOGIC FOR BATTERY CHARGE FROM SOLAR PANEL COUPLED WITH BOOST CONVERTER.

<sup>1</sup>Daniel Alonso Juárez Martínez, <sup>2</sup>Albino Martínez Sibaja, <sup>3</sup> Rubén Posada Gómez  
<sup>1,2,3</sup> Instituto Tecnológico de Orizaba, Veracruz, México.

**Abstract-** The main objectives of this project are the design a Maximum Power Point Tracker (MPPT) using Fuzzy logic to maintain one battery at its maximum power point of charge using a solar panel, the next objective is design a PID controller with a single pole through the method root locus to control a boost topology using the energy stored in a battery to raise it up to 120 V DC, in order to power a system with conventional LED lights.

**Keywords** – Root locus; MPPT; Fuzzy logic; PID with single pole, fuzzification, defuzzification.

## I. INTRODUCTION

Around the world there are zones where electrical energy cannot be obtained from Federal Electricity grid, either because of its Geographic location or because it needs to be portable, as in automobile, a ship, a submarine or a spaceship, therefore, it is necessary to find an alternative source of energy. [1][2].

Of the most promising sources we can find some systems based in eolic and solar energy, although efficiency is low, they are considered acceptable and the most important reason is the great supply of raw material in addition it is clean energy. [3 - 6].

For the management of solar energy currently generated according to the literature a method called *Maximum Power Point Tracker* (MPPT) is used and the technique that has proven the best result is *Fuzzy Logic*. This Method allows to charge a battery more quickly and efficiently, but with the limitation of not exceeding the maximum current supported by the battery [7 -15]. This document describes an electrical power system based on a solar panel of 100 W, which through an MPPT will charge a battery of 12 V, 7Ah and the energy stored will be used by a switched mode power supply boost topology DC to DC and this will meet the lighting needs of a room house. For the design and simulation of the MPPT the software NI LabView 2014 was used, and in the case of the boost topology and the PID Controller with single pole the software NI Multisim 13.0 and Ultiboard 13.0 were used respectively.

## II. MATERIALS AND METHODS

### 1. MPPT.

As a first step we will detail the design of a MPPT using a controller based on fuzzy Logic.

The design of this controller is based on the change of an input variable that can be: Voltage of the Maximum Power Point ( $V_{mpp}$ ) or Current of the Maximum Power Point ( $I_{mpp}$ ) depending on which one is chosen we can estimate the other using fuzzy sets, on this particular case the current of the maximum power point that the battery supports ( $I_{mppb}$ ) and the derivate of ( $I_{mpp}$ ), this current is smaller than the  $I_{mpp}$  produced by the solar panel. The design of this MPPT does not explicitly account for the change of irradiance or temperature as input variables, because it operates between the points of maximum and minimum current produced by the solar panel in the area where it is located within which they are already implicit included. Figure 1 shows the location of the maximum power point of a solar panel or solar cell to which the MPPT will follow each time it changes.

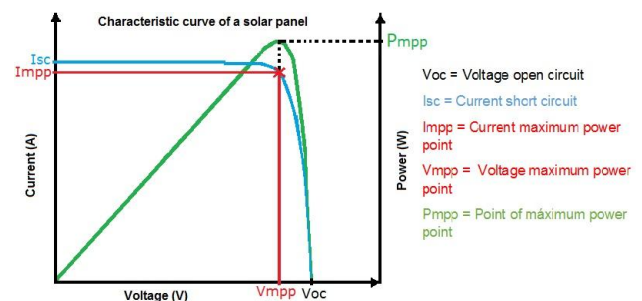


**Figure 1. Location of the maximum power point.**

To sense the current that the battery charges, an ACS712T current sensor of the ALLEGRO company had to be characterized through an instrumentation amplifier.

Knowing the value of the load current between the solar panel and the battery, a controller based on fuzzy logic was designed, that is divided in two stages one of control and one

### Publication History

Manuscript Received : 11 January 2017  
 Manuscript Accepted : 20 January 2017  
 Revision Received : 25 February 2017  
 Manuscript Published : 28 February 2017

of power, the controller has the function of switching 6 resistors having one fixed and the other 5 resistors to be switched in a power stage through the control stage, these switches range from the maximum resistance value to the minimum required to maintain the load current at its maximum power point as long as possible. The output signal of the sensed current is acquired by a hardware platform model ARDUINO MEGA ADK. This signal is sent to the software NI LabView 2014 where it is processed.

The equivalent circuit to the MPPT is shown in the blocks diagram in Figure 2 which detail the control stage and the power stage.

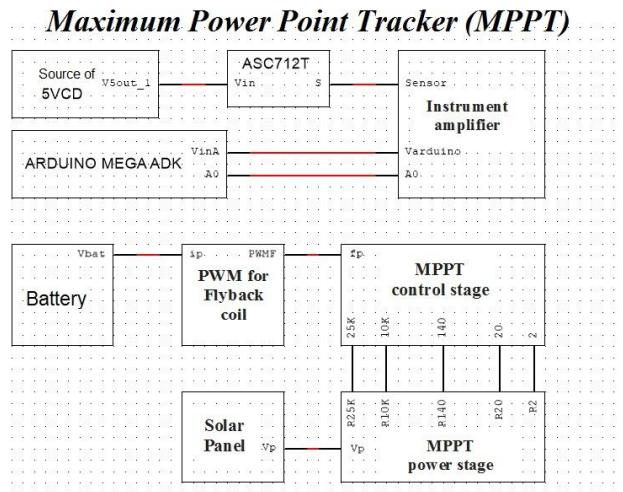


Figure 2. Blocks diagram for MPPT

In the case of the control block a Flyback topology was designed with 5 secondary windings output of 12V of CD, these outputs will provide 5 activation signals for the MOSFET'S of the power stage when determined by the control signal from a fuzzy controller, it will activated solid state relays through the ARDUINO MEGA ADK card.

The design of the power stage is governed by the following equations to locate the maximum power point as far as possible when the weather changes. This action is achieved by modifying the resistance that the battery charges, for this it is necessary to know the values of maximum and minimum voltages of the solar panel and the battery. In this way we can find the minimum and maximum resistance value, through Equation 1 and the Equation 2, between these values can be realized different commutations of resistances by a fuzzy controller in order to maintain the current that charges the battery in the maximum power point.

The values for this fuzzy system were obtained heuristically by proposing 2 values of very large resistances in reference to the Rmax and 3 large values in reference to the Rmin the values in spite of being heuristic values they are obtained through Equation 3 as shown in Table 1.

It is recommended that the switching of these values (increase decreasing limiting resistance) be as linear as possible.

$$R_{min} = \frac{V_{minps} - V_{maxbat}}{I_d} \quad \text{Equation 1}$$

$$R_{max} = \frac{V_{maxps} - V_{minbat}}{I_d} \quad \text{Equation 2}$$

$$R_p = \frac{R_{off}R_{min}}{R_{off} - R_{min}} \quad \text{Equation 3}$$

From Equation 1 is defined:

Rmin	Minimum resistance
Vminps	Minimum Solar Panel Voltage
Vmaxbat	Maximum battery voltage
I <sub>d</sub>	Desired current

From Equation 2 is defined:

Rmax	Maximum resistance
Vmaxps	Maximum Solar Panel Voltage
Vminbat	Minimum battery voltage
I <sub>d</sub>	Desired current

From Equation 3 is defined :

R <sub>off</sub>	Resistance of offset or resistance of the previous parallel.
Rmin	Resistance value to be obtained or the nearest commercial value

Table 1 Resistance values for the power stage

R <sub>off</sub>	3.8 Ω
R1	25 K Ω
R2	10 K Ω
R3	140 Ω
R4	20 Ω
R5	1.5 Ω

Having these values we can define the fuzzy sets for the sensed current I<sub>t</sub> and the derivative of the current dI<sub>t</sub>/dt which integrate the table of sugeno, this process is called fuzzification, as shown in Table 2.

It is important to mention that at the moment of defining fuzzy sets should choose the membership function with which these fuzzy sets work, for this controller will work with a trapezoidal function for the inputs.

**Table 2 Sugeno values**

$\frac{dIt}{dt} / It$	MP	P	I	G	MG
MN	24	16	10	9	4
N	25	19	11	8	3
Z	26	20	12	7	2
P	27	21	13	6	1
MPO	30	23	15	5	0

The numbers shown in decimal base are fuzzy sets called *singletons* used to represent the output variable, at the moment to convert the decimal number to binary we obtain the switching sequence of the solid state relays (control action) this process is called defuzzification. Again it is important to mention that a defocusing method must be chosen. for this controller the method that give the best result was the center of the maximum.

In summary, the table establishes a relation between the inputs and the outputs, that relationship is determined by the user based on the experience acquired by linguistic rules and not of equations as in mathematical models. This is a cognitive activity that allows us to find a solution for a highly nonlinear system such as the power of a solar panel. In the Table 3 it describes the fuzzy sets for It, the same is done in Table 4 for dIt/dt. For the fuzzy sets in the output it is not necessary to display them in a table since it is understood that the decimal number is the switching of the solid state relays.

**Table 3 Fuzzy sets for It.**

Diffuse set name	Description	Range in amper
MP	To smaller	0 a 1.67
P	Smaller	1.68 a 1.86
I	Ideal	1.87 a 2.04
G	Big	2.05 a 2.22
MG	To big	2.23 a 5.56

**Table 4 Fuzzy sets for dIt/dt.**

Diffuse set name	Description	Range in amper
MN	To negative	-5.56 a -1
N	Negative	-0.99 a -0.5
Z	Cero	-0.49 a 0
P	Positive	0.01 a 0.5
MPO	To positive	0.51 a 5.56

To conclude the design of the fuzzy controller, we describe the linguistic rules that define the control action at the output, as shown in Table 5.

**Table 5 Linguistic Rules for MPPT**

1	if "It" is "MP" and "dIt/dt" is "MN" then the output is "24"
2	if "It" is "MP" and "dIt/dt" is "N" then the output is "25"
3	if "It" is "MP" and "dIt/dt" is "Z" then the output is "26"
4	if "It" is "MP" and "dIt/dt" is "P" then the output is "27"
5	if "It" is "MP" and "dIt/dt" is "MPO" then the output is "30"
6	if "It" is "P" and "dIt/dt" is "MN" then the output is "16"
7	if "It" is "P" and "dIt/dt" is "N" then the output is "19"
8	if "It" is "P" and "dIt/dt" is "Z" then the output is "20"
9	if "It" is "P" and "dIt/dt" is "P" then the output is "21"
10	if "It" is "P" and "dIt/dt" is "MPO" then the output is "23"
11	if "It" is "I" and "dIt/dt" is "MN" then the output is "10"
12	if "It" is "I" and "dIt/dt" is "N" then the output is "11"
13	if "It" is "I" and "dIt/dt" is "Z" then the output is "12"
14	if "It" is "I" and "dIt/dt" is "P" then the output is "13"
15	if "It" is "I" and "dIt/dt" is "MPO" then the output is "15"
16	if "It" is "G" and "dIt/dt" is "MN" then the output is "9"
17	if "It" is "G" and "dIt/dt" is "N" then the output is "8"
18	if "It" is "G" and "dIt/dt" is "Z" then the output is "7"
19	if "It" is "G" and "dIt/dt" is "P" then the output is "6"
20	if "It" is "G" and "dIt/dt" is "MPO" then the output is "5"
21	if "It" is "MG" and "dIt/dt" is "MN" then the output is "4"
22	if "It" is "MG" and "dIt/dt" is "N" then the output is "3"
23	if "It" is "MG" and "dIt/dt" is "Z" then the output is "2"
24	if "It" is "MG" and "dIt/dt" is "P" then the output is "1"
25	if "It" is "MG" and "dIt/dt" is "MPO" then the output is "0"

The fuzzy controller designed in the NI LabView 2014 software, using the fuzzy system designed tool is based on the last 4 tables.

Figure 3 shows the fuzzy sets of the sensed current It, as well as their ranges and their membership functions, the Figure 4 shows the same characteristics, but for the fuzzy sets of the derivative of the sensed current, likewise the fuzzy sets of the output variable are shown in Figure 5.

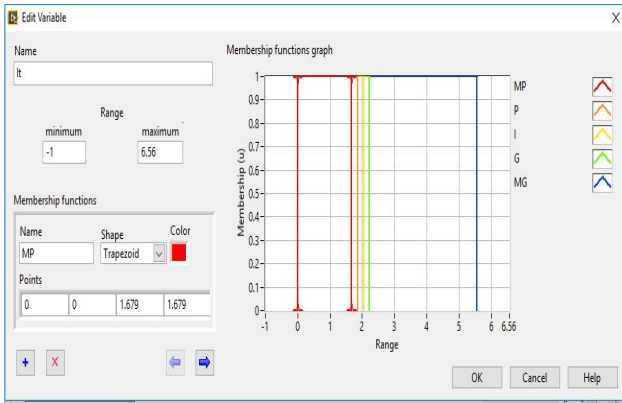


Figure 3. Fuzzy sets for the sensed current

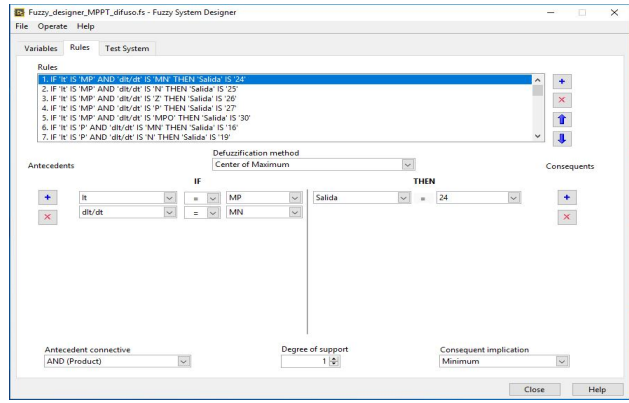


Figure 6. Language rules for the designed system

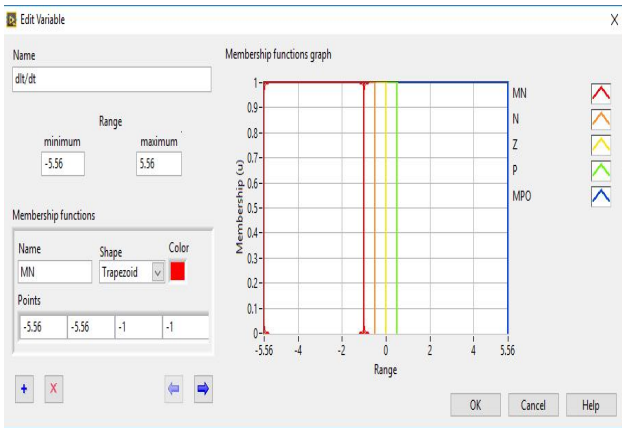


Figure 4. Fuzzy sets for dIt/dt

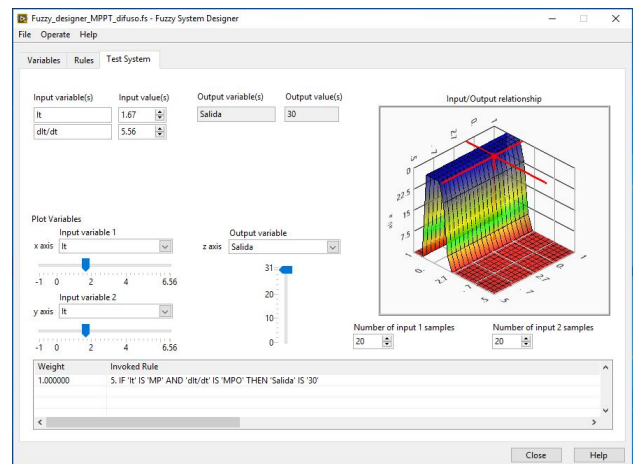


Figure 7. Fuzzy System Designer simulation interface for the fuzzy controller designed.

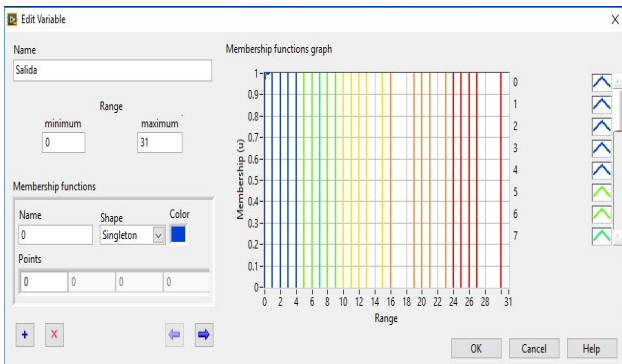


Figure 5. Fuzzy sets for the output variable

After defining the fuzzy sets of the system, the linguistic rules for the control action will be established as shown in Figure 6 and finally a simulation of the controller is carried out, as shown in Figure 7 in the simulation it can be observed that in front of sensed current  $I_t = 1.67$  which is equal to a diffuse set MP and a derivative of the sensed current  $dI_t/dt = 5.56$  which is equal to a fuzzy set MPO, produces an output 30, by linguistic rule number 5.

## 2. Boost converter.

The output from the solar panel is between 18V and 21.9V DC, this will charge a 12 V DC battery through a MPPT. The integration of the solar panel and the battery has as result a partially uninterrupted power source because the generated energy is sensitive to meteorological variations.

Subsequently, it is necessary to use a boost topology, which brings the voltage of the battery from 12 V to 120 V DC, in order to break the barrier of conditioning circuit that is inside the conventional LED lights. Figure 8 shows an electrical diagram of a boost topology

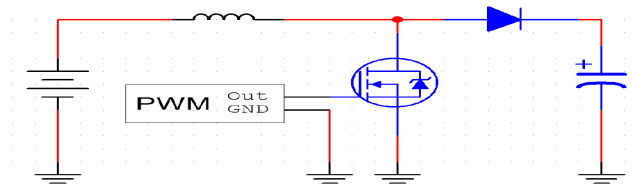


Figure 8. Boost topology

The values of the components presented in Table 6 were taken in consideration for the Boost topology controller design.

**Table 6 Values of components for Boost topology.**

Parameter	Value	Units
<i>L</i>	16.508	<i>mH</i>
<i>R</i>	2448.979	$\Omega$
<i>C</i>	2200	$\mu F$
<i>Vi</i>	12.7	<i>V</i>
<i>Vo</i>	120	<i>V</i>

Where:

*Vi* is considered input voltage provided by the battery.

*Vo* is considered output voltage from Boost topology to the main load.

To obtain the characteristic function of the plant, Equation 5 was used, which also included Equation 4, where:

$$K = \frac{1}{1 - D} \quad \text{Equation 4}$$

$$\frac{Vo(s)}{D(s)} = \frac{KV_i}{LCs^2 + \frac{L}{R}s + 1} \quad \text{Equation 5}$$

<i>Vo(s)</i>	Represents the system's Output.
<i>D(s)</i>	Is the Work Cycle
<i>K</i>	Is the system's gain
<i>Vi</i>	Is the Input voltage
<i>L</i>	Is the designed coil
<i>C</i>	Is the proposed capacitor
<i>R</i>	Is the load resistance which the boost topology is subjected

Once the characteristic function of the plant was obtained, it was applied as the denominator in Equation 5 and replacing the values of the components in the general formula, quadratic equations were obtained, represented as Equation 6 and Equation 7. The location of the plant poles was obtained with this last equation, resulting in the representation shown in Equation 8.

$$LCs^2 + \frac{L}{R}s + 1 = 0 \quad \text{Equation 6}$$

$$s = \frac{-(-0.185606) \pm \sqrt{(-0.185606)^2 - 4(1)(27.53486 \times 10^3)}}{2(1)} \quad \text{Equation 7}$$

$$s = -92.803 \times 10^{-3} \pm 165.94 \quad \text{Equation 8}$$

The definition and calculation of the appropriate controller for the plant was the next step. For the special case of a switched power supply, a single-pole PID controller was used, since this type of controller provided an improvement in the transitory state.

A single-pole PID controller transfer function is shown in Equation 9, where zeros are found in the numerator, while the denominator is composed by the controller poles.

$$Gc(s) = \frac{K \left( \frac{s}{wn_1} + 1 \right) \left( \frac{s}{wn_2} + 1 \right)}{s \left( \frac{s}{wn_3} + 1 \right)} \quad \text{Equation 9}$$

Root Locus method was used for the design of this particular controller. Therefore, an analysis which fulfill the necessary conditions of magnitude was needed, in order to perform the steps below:

1. Calculate the natural frequency of the plant (*wn*) using Equation 10, being *apl* = -92.803<sup>-3</sup> and *bipl* = 165.94 .

$$wn = \sqrt{(apl)^2 + (bipl)^2} \quad \text{Equation 10}$$

2. Calculate the controller frequency, tending to be 10 times faster than the natural frequency of the plant with an angle of almost 60°, these degrees were useful to obtain the location of the poles in closed loop through Equation 11, Equation 12 and Equation 13; these were the poles in closed loop. In this case, a controller 10 times faster than the plant at an angle of 45° was used.

$$wn10 = wn * 10 \quad \text{Equation 11}$$

$$aco = wn10 * \cos 135^\circ \quad \text{Equation 12}$$

$$bico = wn10 * \sin 135^\circ \quad \text{Equation 13}$$

3. Then, the phase analysis was made, in Equation 14, one of the fundamental conditions needed to secure the controller to stay in the stable region of the *S* plane.

$$\alpha 1 + \alpha 2 = -180 + \beta 1 + \beta 2 + \beta 3 + \beta 4 \quad \text{Equation 14}$$

Therefore, the calculation of the angles that formed the poles in closed loop was developed, in relation to the integrator ( $\beta 1$ ) represented in Equation 15, the plant poles; the first pole ( $\beta 2$ ) was obtained with Equation 16 and the second ( $\beta 3$ ) with Equation 17.

For the Zeros; one of them (*Z1*) was proposed relatively close according to the magnitudes of the axis of abscissas, located in -10 for this analysis as is represented in Equation 18. Later, the angle ( $\alpha 1$ ) formed with the poles in closed loop was calculated, as shown in Equation 19.

The second Zero should have been proposed with an angle always lower than  $\beta 1$ , in order to avoid the annulation of the integrative action, and simultaneously, to preserve a relation between the quantity of lacking degrees to accomplish the phase condition, leaving a small but significant magnitude in degrees to add a single pole.



Based on the mentioned above, angle  $\alpha_2$  was established as  $130^\circ$ , presented in Equation 20, and the second zero (Z2) was calculated with Equation 21.

To obtain the location of the single pole, its angle  $\beta_4$  was calculated in first place with Equation 22, and finally the position of the single pole was established with the Equation 23.

$$\beta_1 = 180 + \arctan \left[ \frac{(bico)}{aco} \right] \quad \text{Equation 15}$$

$$\beta_2 = 180 + \arctan \left[ \frac{(bico - bipl)}{(aco - apl)} \right] \quad \text{Equation 16}$$

$$\beta_2 = 180 + \arctan \left[ \frac{(bico + bipl)}{(aco - apl)} \right] \quad \text{Equation 17}$$

$$Z1 = 10 \quad \text{Equation 18}$$

$$\alpha_1 = 180 + \arctg \left[ \frac{bico}{(aco - Z1)} \right] \quad \text{Equation 19}$$

$$\alpha_2 = \beta_1 - 5^\circ \quad \text{Equation 20}$$

$$Z2 = aco - \frac{bico}{\tan \alpha_2} \quad \text{Equation 21}$$

$$\beta_4 = 180 + \alpha_1 + \alpha_2 - \beta_1 - \beta_2 - \beta_3 \quad \text{Equation 22}$$

$$PS = aco - \frac{bico}{\tan \beta_4} \quad \text{Equation 23}$$

The phase condition can be seen widely in Figure 9, where the elements calculated and proposed are shown.

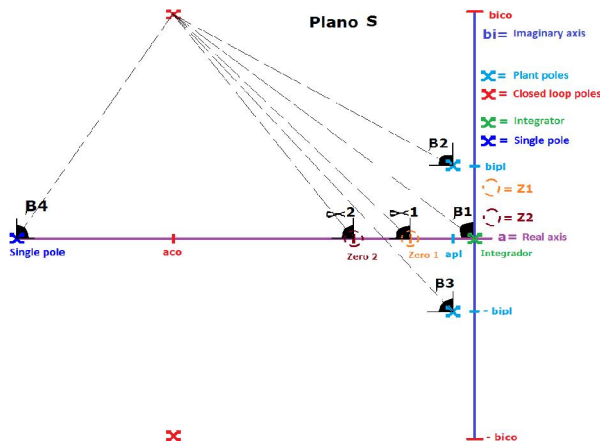


Figure 9 S Plane of a single pole PID controller

- Subsequently, the analysis for the magnitude condition was made, which hasn't reached over 100, as shown in Equation 24, to maintain the controller in the stable region of the S plane.

$$K \leq 100 \quad \text{Equation 24}$$

For the calculation of the magnitude, variable K was isolated of the equation that determined the magnitude condition, as can be seen in Equation 25.

$$|Gc(s)G(s)H(s)| = K \left[ \left[ \frac{s}{wn_1} + 1 \right] \left[ \frac{s}{wn_2} + 1 \right] \right] \left\{ [PWMD] \left[ \frac{V_i}{As^2 + Bs + C} \right] \left[ \frac{SP}{Vo} \right] \right\} = 1 \quad \text{Equation 25}$$

From the Equation 25, can be found:

- Gc(s) Representing the single pole PID controller block
- G(s) Representing the plant block (Boost topology)
- H(s) Representing the control loop block (conditioning circuit)
- wn1 Representing the location of the first Zero (Z1)
- wn2 Representing the location of the second Zero (Z2)
- wn3 Representing the location of the controller's single pole (PSC)
- PWMD Representing the typical voltage of the PWM to be proven in open loop, this way made possible to select a work cycle that secures the wanted output voltage, as is shown in Figure 10
- A Representing the quadratic term of the plant's characteristic equation
- B Representing the lineal term of the plant's quadratic equation
- C Representing the independent term of the plant
- SP TL494 set voltage for switched power supplies, as manifested in Figure 10
- Vo Representing desired output voltage of the Boost topology
- Vi Representing input voltage of the Boost Topology

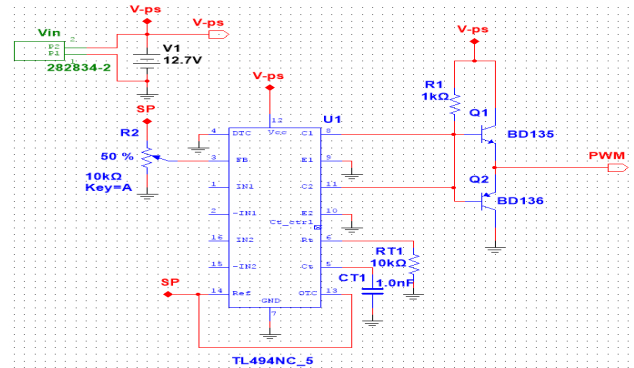


Figure 10 Opened Loop Controller

A recommendation is made for designers to calculate the magnitudes for each element in the controller, the plant and the conditioning circuit, in the benefit to obtain one single coefficient that represents the magnitude of each block, making easier to isolate the variable K.

In this way, K became possible to obtain using the Equation 26.

$$K = \frac{1}{|Gc(s)| * |G(s)| * |H(s)|} \quad \text{Equation 26}$$

In Table 7 the values obtained for the phase condition ( $\alpha_1, \alpha_2, \beta_1, \beta_2, \beta_3, \beta_4, Z_1, Z_2, PS$ ), the magnitude (K), the poles in closed loop (PLC) and the poles of the plant (s) are exposed.

**Table 7 Calculated values for a single pole PID controller using Root Locus method**

$\alpha_1$	133.7528435420227°
$\alpha_2$	130°
$\beta_1$	135°
$\beta_2$	163.6689298591416°
$\beta_3$	120.3513120320442°
$\beta_4$	24.732601650836813°
Z1	-10
Z2	-37.758389914668385
PS	-744.1134413361763
K	45.827407063973844
PLC	-234.669380753692±234.669380753692i
s	-0.092803030296843±165.93628451685i

Once the conditions of phase and magnitude are accomplished, a simulation of the system's response in the domain of time should be made, to facilitate a determination of the transitory state and its stability (Figure 11), where the axis of abscissas must show the time in seconds and the axis of ordinates must show the output voltage of the system.

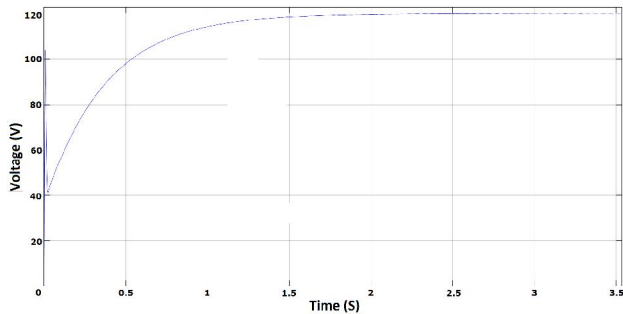


**Figure 11. System's response in the domain of time**

After a satisfactory response was obtained by simulating the system, the calculation of the components which integrate the single pole PID controller took place and was reflected in Figure 12. The controller stood defined by the Equation 27, where Zf was obtained by the Equation 28, and Z1 was obtained by the Equation 29. To make possible an equivalence in the single pole PID controller structure, to express all the equation in a simpler form was needed. This is the reason why the Equation 28 and Equation 29 were simplified in Equation 30 for Zf and Equation 31 for Z1.

Equation 30 and Equation 31 were replaced in Equation 27, as shown in Equation 32. From this equation, three steps of simplification were done with the aim to adjust Equation 32 in a single pole PID controller structure. The first step resulted in Equation 34, and the third step resulted in Equation 35.

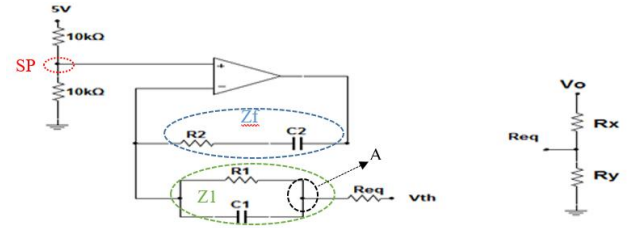


**Figure 12 Single pole PID controller electronic circuit**

$$G_c(s) = \frac{Z_f}{Z_1} \tag{Equation 27}$$

$$Z_f = R_2 + \frac{1}{sC_2} \tag{Equation 28}$$

$$Z_1 = Req + \frac{R_1 \left( \frac{1}{sC_1} \right)}{R_1 + \frac{1}{sC_1}} \tag{Equation 29}$$

$$Z_f = \frac{sR_2C_2 + 1}{sC_2} \tag{Equation 30}$$

$$Z_1 = \frac{sReqR_1C_1 + Req + R_1}{sR_1C_1 + 1} \tag{Equation 31}$$

$$G_c(s) = \frac{Z_f}{Z_1} = \frac{\frac{sR_2C_2 + 1}{sC_2}}{\frac{sReqR_1C_1 + Req + R_1}{sR_1C_1 + 1}} \tag{Equation 32}$$

$$G_c(s) = \frac{(sR_1C_1 + 1)(sR_2C_2 + 1)}{(sC_2)[s(ReqR_1C_1) + Req + R_1]} \tag{Equation 33}$$

$$G_c(s) = \frac{(sR_1C_1 + 1)(sR_2C_2 + 1)}{(sC_2)(Req + R_1) \left[ s \left( \frac{ReqR_1}{Req + R_1} \right) + 1 \right]} \tag{Equation 34}$$

$$G_c(s) = \left[ \frac{1}{C_2(Req + R_1)} \right] \left[ \frac{(sC_1R_1 + 1)(sC_2R_2 + 1)}{s \left[ s \left( \frac{ReqR_1C_1}{Req + R_1} \right) + 1 \right]} \right] \tag{Equation 35}$$

Equivalences were established through these equations, for the magnitude (K) as shown in Equation 36, for the location of the first zero (Z1) with Equation 37, for the location of the second zero (Z2) with Equation 38, for the location of the single pole (PS) with Equation 39; although, for the integrator there were no direct equivalence, it was implicated in the electronic circuit shown in Figure 12.

$$K = \frac{1}{C_2(Req + R_1)} \tag{Equation 36}$$

$$R_1C_1 = \frac{1}{wn1} \tag{Equation 37}$$

$$R_2C_2 = \frac{1}{wn2} \tag{Equation 38}$$

$$\frac{ReqR_1C_1}{Req + R_1} = \frac{1}{\omega n_3} \quad \text{Equation 39}$$

Once equivalences were assigned according to the single pole PID controller, the following sequence should be done:

1. One of the capacitors must be proposed, it is recommended to propose capacitor C1 facilitating resistance R1 calculation, as illustrated in Equation 40.
2. R1 must be isolated from Equation 37, as shown in Equation 41, replacing C1 value.
3. Variable Req must be isolated from Equation 39 and R1 and C1 values previously obtained must be replaced, as marked in Equation 42.
4. Draw from the Req value, Rx and Ry can be calculated, using the Thevenin theorem, as witnessed graphically in Figure 13, obtaining a Thevenin voltage (voltage in node A) through Equation 43; It is important to mention that Thevenin voltage will be capable to reach a maximum value of 2.5 V when the output in boost topology (Vo) achieves the desired voltage, resulting in a regulation of the work cycle at the TL494 PWM output, calculations must be made with the maximum Thevenin voltage value. After the Thevenin theorem has been applied, another way to calculate Req is obtained if the Rx and Ry values were previously acquired, as shown in Equation 44.

From Equation 43 and Equation 44, the denominator must be isolated as exemplified in Equation 45 and Equation 46, searching to equate them and obtain Equation 47, from which Rx can be isolated, as demonstrated in Equation 48. Ry can be isolated from any of these equations: Equation 44, Equation 45, Equation 46 or Equation 47, and once isolated, can be replaced the value obtained for Rx. For this case, Ry can be calculated with Equation 49.

5. For capacitor C2 calculation, C2 variable must be isolated in Equation 36 as shown in Equation 50, then, K, Req and R1 values must be replaced, previously calculated.
6. Resistance R2 calculation must be obtained by isolating R2 in Equation 38 as established in Equation 51, and replacing C2 value.

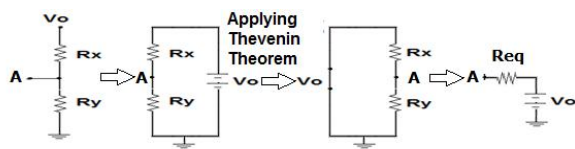


Figure 13. Thevenin theorem applied to node A

$$C1=509 \text{ nF} \quad \text{Equation 40}$$

$$R_1 = \frac{1}{\omega n_1 C_1} \quad \text{Equation 41}$$

$$Req = \frac{R_1}{R_1 C_1 \omega n_3 - 1} \quad \text{Equation 42}$$

$$V_{th} = \frac{V_o R_y}{R_x + R_y} \quad \text{Equation 43}$$

$$Req = \frac{R_x R_y}{R_x + R_y} \quad \text{Equation 44}$$

$$R_x + R_y = \frac{V_o R_y}{V_{th}} \quad \text{Equation 45}$$

$$R_x + R_y = \frac{R_x R_y}{Req} \quad \text{Equation 46}$$

$$\frac{R_x R_y}{Req} = \frac{V_o R_y}{V_{th}} \quad \text{Equation 47}$$

$$R_x = \frac{V_o Req}{V_{th}} \quad \text{Equation 48}$$

$$R_y = \frac{R_x V_{th}}{V_o - V_{th}} \quad \text{Equation 49}$$

$$C2 = \frac{1}{K(Req + R1)} \quad \text{Equation 50}$$

$$R2 = \frac{1}{\omega n_2 C2} \quad \text{Equation 51}$$

In Table 8, the values obtained for the components which integrate a single pole PID controller are enlisted.

Table 8 Values of the components for single pole PID controller integration using an IC TL494

Parameter	Value
C1	509 nF
R1	196.46 KΩ
Req	2.6762 KΩ
Rx	128.46 KΩ
Ry	2.7331 KΩ
C2	109.58 nF
R2	241.7 KΩ

Finally, an image of the circuits designed and manufactured of the proposed system are shown. For the case of the battery and the bulbs were acquired. To the left there are the MPPT and the PCB in red it is the control stage and is coupled to the power stage.

The boost converter is located on the right it integrates the PID controller and the boost topology and in the top is the test bench of illumination, as show in the figure 14.



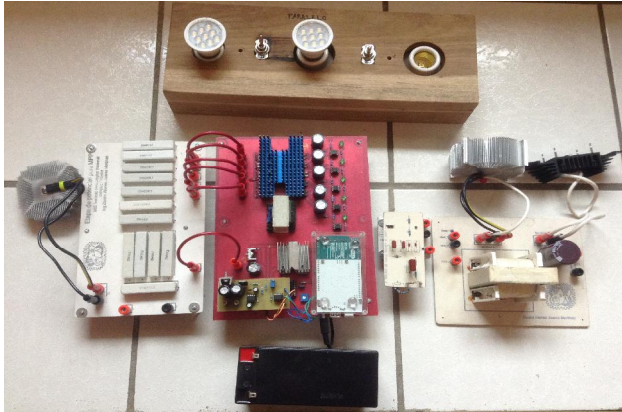


Figure 14 PCBs designed device

### III. CONCLUSIONS

The conditioning circuits developed have been successfully implemented leads to more complex circuits such as a boost converter and a maximum power point tracker, which gives place to the proposed electrical system. These circuits are described in detail below.

#### Boost converter.

In this document, an elevator source was designed with the purpose of generating an alternative to work with lighting based on LED technology available in the market. The need arises that this technology only exists for use of AC, therefore, based on the assumption that the LED technology works with DC, by raising the voltage up to 120 V DC. It was possible to activate the device without the need to transform the voltage into AC. This is reflected economically as acquiring LED bulbs that work with 120 V AC is cheaper than buying special bulbs for solar panels.

#### Maximum power point tracker.

In order to be able to occupy the energy generated by the solar panel, the maximum power point tracker (MPPT) was integrated to intelligently charge the battery through a fuzzy logic controller, which varies the current charged by the battery, while there is enough sunlight. The designed controller was manufactured with a relatively low cost and is parameterizable in this way if it is necessary to scale the system to a higher power only the power stage must be modified, allowing maximum use of the generated energy.

### REFERENCES

- [1] M. F. Alvarez Mendoza, "Modelado y simulación de un sistema híbrido: Eólico-Celda de combustible con generación y almacenamiento de hidrógeno.," 2013.
- [2] A. Kashefi Kaviani, G. H. Riahy, and S. M. Kouhsari, "Optimal design of a reliable hydrogen-based stand-alone wind/PV generating system, considering component outages," *Renew. Energy*, vol. 34, no. 11, pp. 2380–2390, 2009.
- [3] J. C. Gomez, D. Tourn, S. Nesci, and G. R. Zamarillo, "PV cells protection by using class PV fuses," *IEEE Lat. Am. Trans.*, vol. 11, no. 1, pp. 531–537, 2013.

- [4] M. G. Perez Vielma, "Diseño e implementación de un sistema para adquirir las variables energéticas y monitoreo en línea de un sistema híbrido solar-hidrógeno-celda de combustible.," 2011.
- [5] P. M. Molto, T. Jose, and C. J. Vilaplana, "Sistema de producción de hidrógeno y de energía eléctrica a partir de energía fotovoltaica.," no. 4, 2009.
- [6] J. C. Turnbull, C. Sweeney, A. Karion, T. Newberger, S. J. Lehman, P. P. Tans, K. J. Davis, T. Lauvaux, N. L. Miles, S. J. Richardson, M. O. Cambaliza, P. B. Shepson, K. Gurney, R. Patarasuk, and I. Razlivanov, "Toward quantification and source sector identification of fossil fuel CO<sub>2</sub> emissions from an urban area: Results from the INFLUX experiment," *J. Geophys. Res. Atmos.*, vol. 120, pp. 292–312, 2015.
- [7] R. Galán, a. Jiménez, R. Sanz, and F. Martía, "Control Inteligente," *Intel. Artif.*, vol. 4, no. 10, 2000.
- [8] A. Wiesner, R. Diez, and G. Perilla, "Design and implementation of a Buck converter with MPPT for battery charge from solar module," *2013 Power Electron. Power Qual. Appl. PEPQA 2013 - Proc.*, 2013.
- [9] M. A. Eltawil and Z. Zhao, "MPPT techniques for photovoltaic applications," *Renew. Sustain. Energy Rev.*, vol. 25, pp. 793–813, 2013.
- [10] C. L. Liu, J. H. Chen, Y. H. Liu, and Z. Z. Yang, "An asymmetrical fuzzy-logic-control-based MPPT algorithm for photovoltaic systems," *Energies*, vol. 7, no. 4, pp. 2177–2193, 2014.
- [11] Syafaruddin, E. Karatepe, and T. Hiyama, "Polar coordinated fuzzy controller based real-time maximum-power point control of photovoltaic system," *Renew. Energy*, vol. 34, no. 12, pp. 2597–2606, 2009.
- [12] S. Subiyanto, A. Mohamed, and M. A. Hannan, "Intelligent maximum power point tracking for PV system using Hopfield neural network optimized fuzzy logic controller," *Energy Build.*, vol. 51, pp. 29–38, 2012.
- [13] C. Ben Salah and M. Ouali, "Comparison of fuzzy logic and neural network in maximum power point tracker for PV systems," *Electr. Power Syst. Res.*, vol. 81, no. 1, pp. 43–50, 2011.
- [14] M. H. RASHID, *ELECTRÓNICA DE POTENCIA*, CUARTA EDI. MÉXICO, 2015.
- [15] S. Russell and P. Norvig, *Inteligencia Artificial. Un enfoque moderno. 2da Edición.* 2004